ADVANCED AERODYNAMICS AND ACTIVE CONTROLS FOR A NEXT GENERATION TRANSPORT*

A. Brian Taylor
Douglas Aircraft Company

SUMMARY

Studies and developments for the Douglas DC-X-200 are described. In aerodynamics, the use of new and flexible tools for the design of supercritical wings is discussed. Trends in the design and performance of high-lift devices are outlined. In the field of active controls, the determination of suitable configurations with regard to flying qualities is described, particularly related to results from a piloted simulation.

INTRODUCTION

By the nature of today's market pressures, the next generation of transports will require a substantial technical advance. At the same time, the introduction of new technology must be guided both by sound economic guidelines and technical acceptance by operators and regulatory bodies. At Douglas, studies for the next generation medium-range transport have focused on the DC-X-200. The DC-X-200, shown in figure 1, is a major derivative of the DC-10, which is an "energy efficient" transport of its generation.

During studies of the DC-X-200, the NASA Aircraft Energy Efficiency (ACEE) program was introduced to accelerate the incorporation of new technology. The ACEE Energy Efficient Transport (EET) program was directed toward the application of advanced aerodynamics and active controls. This effort has been a useful stimulus to development on the DC-X-200 of concepts where promising advances were offered, and where previous cooperative work with NASA had been enjoyed.

The subsequent selection of tasks encompassed the following:

- Aerodynamics: The design and wind tunnel development of high-aspect-ratio supercritical wings. These tasks investigate the cruise speed regime and also high-lift development. Activities combine Douglas and NASA support.

- Configuration Design: The optimized design of a high-aspect-ratio supercritical wing and winglet combination. This work is still in a formative stage and is not discussed further in this paper.

- Active Controls: The determination of criteria, configuration, and flying qualities associated with augmented longitudinal stability of a level likely to be acceptable for the next generation transport; and the design of a practical augmentation system. These activities also combine Douglas and NASA support. In this paper, aspects of the flying qualities investigation will be discussed.

*Including work performed partially under NASA Contract NAS1-14744.

The gains predicted for these concepts can be evaluated in a number of ways. Two simple but effective measures are the improvements in direct operating cost (DOC) and fuel usage. DOC is one measure of the economics of the aircraft to which the particular technology concept contributes. Fuel reductions relate to energy efficiency.

The true quantification of the gains involves a complete aircraft configuration analysis, in which the relationships of all the factors may be represented. Such an analysis is beyond the scope of this paper. Instead, the effects of each concept will be noted independently.

The initially estimated goals for these concepts are shown below:

	Percent Reduction Relative to DC-10 Technology	
Concept	DOC	Fuel Burned
High-Aspect-Ratio Supercritical Wing	4.5	9.0
High-Aspect Ratio	(1.0)	(4.0)
Supercritical Wing	(3.5)	(5.0)
Advanced High-Lift System	1.9	1.5
Augmented Stability	0.5	1.7

The improvements in both DOC and fuel usage for each concept are substantial. Those associated with the high-aspect-ratio supercritical wing are the largest. The estimation is based on the assumption of high-lift system of the conventional standard which will be described later in the paper. An advanced high-lift system, when applied to this wing, results in a fuel reduction which is significant although smaller than that of the basic wing design. The reduction in DOC is important. As an additional benefit, the advanced high-lift system offers improvement in field length and community noise. The augmented stability derives its benefits from a smaller tail and reduced trim drag. The gains shown here reflect a conservative and low-risk design, but nevertheless are attractive. The technology of active controls is emerging, and a full evaluation of the benefits in this application must await the completion of the current study.

The starting point for the cooperative portions of the high-aspect-ratio wing development was a NASA test in May of 1977. This was followed by an intensive Douglas-funded effort for the design of modified wings to be tested in the EET program. These tests will occur throughout 1978. The high-lift design work is also funded by Douglas. The EET program sponsors both evaluation tasks and the wind tunnel tests which will be conducted in 1978.

The stability augmentation system study was initiated with Douglas funds. An extensive piloted simulation program which explored flying qualities has been completed. The augmentation system design is continuing and will be tested in an extensive piloted simulation early in 1978.

SYMBOLS AND NOMENCLATURE

Values are given in SI and U.S. Customary units. Measurement and calculations were made in U.S. Customary units.

$\mathcal{C}_L$	Aircraft centerline
C_L	Lift coefficient
$C_{L_{MAX}}$	Maximum lift coefficient
C_p	Pressure Coefficient
L/D	Lift-to-drag ratio
MAC	Mean aerodynamic chord, used nondimensionally
OWE	Operational empty weight, kg (lb)
PIO	Pilot-induced oscillation
TOFL	Takeoff field length, m (ft)
TOGW	Takeoff gross weight, kg (lb)
$V_{APPROACH}$	Landing approach speed, m/s (KEAS)
VCK	Variable Camber Krueger, a type of leading edge flap
V_{STALL}	Stall speed at a given configuration, m/s (KEAS)
θ/θ_c	Ratio of pitch attitude to pitch attitude commanded (closed loop resonance), expressed in dB

HIGH-ASPECT-RATIO SUPERCRITICAL WING – HIGH-SPEED DEVELOPMENT

The development of the high-aspect-ratio wing for the DC-X-200 has resulted from advances in technology closely applied to aircraft configuration analyses and trade studies. This section will emphasize aspects of the wing design with reference to those configuration considerations which have posed significant problems.

Development and Configuration Considerations

The wing design has utilized both two-dimensional and three-dimensional high Reynolds number data on supercritical wings obtained by Douglas over the past 10 years, as well as data provided by Dr. R. T. Whitcomb's work at NASA Langley (reference 1). However, the wing of the DC-X-200 differs

from today's standard, as typified by the DC-10, not only in its airfoil design, but also in the manner in which the design philosophy and other advanced technologies impact the overall configuration. An example of these interactions and their effects on the wing design can best be shown by the impact of just two of these variables – the requirement for fuel conservation and the incorporation of an advanced high-lift system. The requirement for minimum fuel dictates a configuration where the advantage of the supercritical airfoil is taken out in a wing which is thicker and has a higher aspect ratio than that of today's transports. The higher aspect ratio, in turn, requires that the wing be designed to higher lift coefficients so that the full potential of the aspect ratio can be used. For example, the C_L for optimum cruise for a typical conventional wing with an aspect ratio of 7 is 0.49. For a high aspect ratio of 10.5, typical of the DC-X-200 designs, the optimum C_L is nearly 0.6.

The impact of the advanced high-lift system on this design is the allowance of a smaller wing area. This combination of a relatively small wing spread over a larger span produces the most difficult problems of the wing design and design integration. Integration introduces requirements for structure and the housing of landing gears, which result in the aft extension of the small chord at the fuselage side and in a large inboard trailing edge extension. Two additional features, in themselves favorable to fuel conservation, compound the problem by requiring an aft movement of the landing gear relative to the wing. These features are the wing-mounted, high-bypass-ratio engines and the relaxed static stability. Figure 2 shows a planform comparison of the DC-10 and a DC-X-200 type wing, and indicates the landing gear locations. The landing gear location is approximately 7 percent further aft on the high-aspect-ratio wing. During the early development of the DC-X-200 wing, the size of the inboard trailing edge extension caused an effective loss of sweep over the inboard wing and difficulties at the trailing edge kink.

Wing Design

Because of the sensitivity of wing weight on fuel requirements and direct operating cost, obvious solutions to the design integration problems such as in increased wing area were rejected in favor of a solution which would not jeopardize the economics or fuel efficiency of the aircraft.

With this objective in mind, an extensive study was undertaken to define the configurations to be tested during 1978. In addition to wind tunnel data, the theoretical analyses included considerable use of a Douglas-developed version of the Jameson 3-D transonic method published in reference 2.

Figures 3 and 4 indicate the breadth of configuration analysis contained in the definition of the wings for the EET models. They also indicate the flexibility and design capability of the Douglas-Jameson program. The test configurations are wings W_3, W_4 and W_5. Figure 3 shows the first half of the entire matrix that evolved during the development of the test wing designs. Figure 4 shows the second half. The study baseline was wing W_A, a configuration closely resembling the configurations W_1 and W_2 from a previous cooperative test program. The initial configuration proved to have inadequate transonic performance as a result of the large trailing-edge break and the airfoil sections. Perturbations and variations in twist, planform, and airfoil sections were therefore examined. Some of these perturbations were imposed by aircraft configuration and system studies.

One of the more interesting developments that resulted from the study is the effect of a small leading-edge glove on the inboard shock development. Figure 5 shows isobar plots (lines of constant pressure) provided by the program. Isobars for the wing with no glove illustrate a concentration of

lines representing a shock wave near the midchord. Significant upsweeping of the shock is evident at the root. With the leading-edge glove added, the shock is significantly weakened. Similar effects have recently been verified experimentally by Dr. Whitcomb.

Figure 6 illustrates the improvement in the upper-surface pressure distribution between the initial baseline W_A and the first test wing W_3. The strong aft shock evident in the W_A pressure distribution has been suppressed and its position brought significantly farther forward.

After completion of the design for wing W_3, a more detailed analysis indicated that buffet C_L could be substantially improved with a planform and twist modification. The primary variation in planform was to extend the chord at the outboard trailing-edge break. An upper-surface pressure distribution at 0.8 semispan is compared with that for wing W_3 in figure 7. The Mach number ahead of the shock is suppressed further, and the shock is moved significantly farther forward to allow the boundary layer a better chance to recover to the airfoil trailing edge.

Further performance potential has been indicated for wing W_5. Its airfoils included a reduced leading-edge thickness to address sensitivity to premature drag creep before drag divergence. Furthermore, the test configuration will investigate the effect of increased aft camber. This characteristic tends to improve buffet C_L, provided viscous effects do not cause excessive losses. The test configurations will enable the leading edge of wing W_4 to be combined with the trailing edge of W_5 and vice versa. Hence, the effects of the leading-edge and trailing-edge modifications can be evaluated separately as well as together. The predicted effect of the leading-edge and trailing edge modifications is indicated in figure 8. The reduced leading-edge thickness suppresses the C_p plateau level ahead of the weak shock which exists at approximately 40-percent chord on wing W_4. The increased aft camber increases the C_p plateau level in the aft region.

Figure 9 shows the estimated percent buffet C_L improvements for wings W_4 and W_5 relative to wing W_3. An approximate improvement of 6 percent is shown for W_4, while a 9-percent improvement is indicated for W_5.

Experimental Development

It is important for proper experimental assessment of the higher cambered supercritical airfoils to have a high Reynolds number capability. This need is enhanced by the relatively small chords associated with the high aspect ratio. For this reason, the NASA Ames 11-foot transonic wind tunnel will be used in the development testing.

The test model consists of components of the DC-X-200 design. The model includes the fuselage, nacelle installations, wing configurations, and the tail surfaces. The horizontal stabilizer has variable incidence capability. Pressure instrumentation will be included in the wing.

HIGH-ASPECT-RATIO SUPERCRITICAL WING – HIGH-LIFT DEVELOPMENT

It may seem self-evident that advances in high-lift systems will be justifiable for a new transport, but the choices need careful consideration. Furthermore, their development for supercritical wings is not yet completed. The promise of increased fuel savings, reduced noise characteristics, and improved

economics must be determined in the context of aircraft configuration studies and validated by design analyses, test, and evaluation. These activities have indicated customer requirements and appropriate mechanical systems which appear to satisfy these requirements. The verification process is to design and test a high-lift development model for the configuration which incorporates supercritical airfoil technology, a high-aspect-ratio wing, and augmented longitudinal stability.

The aerodynamic design of the advanced high-lift system for the wind tunnel model has been based on two- and three-dimensional analysis techniques and related experimental results. Combined potential and viscous programs have been utilized to design the high-lift shapes, with the experimental data base as a guide to acceptable pressure peaks and gradients.

Comparison With a Current Wide-Body Transport

Significant low-speed performance gains may be shown for the advanced configuration compared with current wide-bodied transports. These gains result from the increased aspect ratio, supercritical airfoil, and the high-lift system just described. For example, in takeoff lift-to-drag ratios (L/D), there is a 32 percent increase at the respective 1.2 V_{STALL} limit. This is accompanied by a 50-percent increase in $C_{L_{MAX}}$ for the takeoff flap deflections. Such substantial increases in performance result in reduced flyover noise and smaller takeoff field length requirements when compared to existing aircraft.

Because the approach noise condition is often more critical, the improvement in landing performance is even more significant. The design indicates a large increase in approach L/D, figure 10. For a 1.3 V_{STALL} condition the increase in L/D is approximately 44 percent. The $C_{L_{MAX}}$ increase for the advanced configuration is approximately 30 percent larger.

Impact of the High-Lift System Alone

A comparison of the effect of the high-lift systems alone is also of value. For this comparison, aircraft configurations with, respectively, a conventional and an advanced high-lift system have been formulated. The configurations both utilize the aspect ratio, planform, and airfoil of the W_A wing previously described.

The conventional and advanced configurations are shown in figure 11. The conventional system utilizes a circular arc motion trailing-edge vane flap and a leading-edge slat. The inboard and outboard flap systems are separated by a high-speed aileron which is undeflected in the high-lift mode. The selected advanced high-lift components include an inboard and outboard two-segment flap system. A flaperon, which is deflected during takeoff and landing, is located between the inboard and outboard flaps. The leading-edge high-lift device is an inboard and outboard Variable Camber Krueger (VCK). At low speed the lateral control is obtained by an aileron, which extends from the outboard flap to the wing tip, and spoilers. Chordwise sections are shown in figure 12.

For the $C_{L_{MAX}}$ variation with flap deflection, the advanced system indicates a gain of approximately 20 percent for the various flap deflections (figure 13). The improved $C_{L_{MAX}}$ is due to the larger flap extension, the increased high-lift capability of the leading-edge device, and the increments in lift due to the flaperon deflection.

The change in takeoff L/D characteristics between the advanced and conventional high-lift systems is shown in figure 14. The L/D curves presented are determined by the envelope of L/D for various flap deflections which would be used in the takeoff mode. An 11-percent gain in L/D is shown at the largest C_L values. At the maximum C_L value for the conventional high-lift system, an increase in L/D of 23 percent is indicated.

Figure 15 indicates that for landing approach, incorporation of the advanced system increases the approach L/D by some 18 percent, and this figure would result in significant reduction in the critical area of approach noise. A more uniform span load distribution with the deflection of the flaperon and the improved drag characteristics of the advanced high-lift components are two sources of the improvement in L/D characteristics.

The design range for the evaluation aircraft is 5556 km (3000 n mi). At this range, a savings of 0.6 percent of fuel burned is obtained by the configuration incorporating the advanced system relative to the one using the conventional system. More significant, however, is the stage length at which the aircraft is most commonly to be used. The average stage length is expected to be 1389 to 1852 km (750 to 1000 n mi). At these ranges, fuel savings on the order of 1.6 to 1.3 percent, respectively, are indicated.

The results of the sizing comparison are shown in table 1. Takeoff weight, operational empty weight, and wing area are the configuration characteristics represented. The conventional configuration is sized by the approach speed requirement, leading to an initial cruise altitude slightly larger than the mission requirement of 10,363 meters (34,000 feet). The advanced configuration is sized by this requirement. The resulting approach speed is nearly 3 m/s (5 KEAS) less than the mission requirement. The respective wing areas are approximately the same size. However, the advanced configuration has a significantly reduced takeoff field length. Moreover, the improved L/D characteristics will reduce noise levels for both takeoff and landing operations.

Experimental Development

The wind tunnel tests are planned for the Ames 12-foot facility. This tunnel offers the high Reynolds Number capability of nearly 2 million per meter (6 million per foot) which is considered important in developments of this nature. Furthermore, the tunnel offers a Mach number sweep capability.

The configuration selected for test reflects the advanced system with the refined wing planform and airfoil sections previously described, and is illustrated in figure 16. High-lift components will include capability for changes in deflection and position. A low-speed aileron and spoilers are also included in the model components. The wind tunnel model will include pressure instrumentation on the wing and high-lift components.

AUGMENTED LONGITUDINAL STABILITY SYSTEM STUDY

Augmented stability in the DC-X-200 is aimed at matching the known and satisfactory handling qualities of the DC-10, when augmented, and provision of a satisfactory level of handling when unaugmented. In spite of the current rapid progress in active controls, there is much in this field still to be studied and understood. The Douglas EET activity, therefore, covers the design tasks with a thorough and disciplined study.

The study contains three distinct elements. The first is the formulation and verification of the aerodynamic data and flying qualities criteria, the determination of quantitative reliability requirements and the synthesis of the augmentation control laws. The flying qualities and configuration effects have been studied in detail, the study culminating in a piloted simulation in a six-degree-of-motion facility. Only the investigations concerning flying qualities will be discussed in this paper. The second element is the system configuration study consisting of the formulation, analysis, and selection of an architecture and then evaluation of the augmented aircraft. The third element consists of the estimations of the potential fuel savings, the verification of compliance with the proposed safety criteria, and the determination of the impact of relaxed stability on the aircraft certification. The second element is well advanced and will include, later this year, an elaborate simulation and evaluation on the six-degree-of-motion stimulator. The third element also is underway.

Scope of the Flying Qualities Work

The establishment of minimum acceptable levels of stability has been the subject of numerous investigations. A suitable solution requires the development and acceptance of evaluation criteria, a careful definition of the configuration characteristics, the prepararation of a realistic simulation model, and a comprehensive pilot evaluation.

Adequate evaluation needs a comprehensive data base. Very little useful data from wind tunnels are available for this type of configuration. Therefore, aerodynamic data were generated by analytical means and put in the form of linearized small-perturbation equations. These equations have been used primarily for control system design. Full flight-envelope equations were developed for use in the motion-base simulation. The extent of the representation has, it is believed, enabled a thorough exploration of flying qualities on the simulator.

The test was conducted on the Douglas six-degree-of-freedom motion simulator system which supports a complete simulated cockpit and provides realistic motion cues. The cockpit simulator is attached to a base supported by six hydraulic jacks. This configuration, shown in figure 17, has the arrangement developed by the Franklin Institute, with an improved performance unsurpassed by any system for the simulation of transport aircraft motion. Visual simulation for the cockpit is available from a Redifon visual flight attachment.

On the simulator, flying qualities of the unaugmented aircraft were examined through most of the flight envelope. This examination led to emphasis being placed on the cruise flight and landing approach conditions. Five test pilots, experienced in DC-10 and other transport handling evaluations, participated in the experiment.

Flying Qualities Criteria

Criteria for flying qualities must be applied in two cases. The first is the case of the unaugmented vehicle, where total augmentation system failure has occurred. The second case is with the augmentation system in normal operation.

In the first case, acceptable unaugmented qualities are determined by safety considerations. It is usual for these to be given in terms of either Cooper-Harper pilot rating values (reference 3) or the military

flying qualities "levels" (reference 4). Safety considerations for commercial transport aircraft dictate a maximum acceptable pilot rating of 6.5, which corresponds approximately to Level 2 from the military specification. In the second case, the desired flying qualities of the normal augmented aircraft are military Level 1, which corresponds to a pilot rating of 3.5 or better.

At the outset of the work, it was decided that satisfactory (Level 1) flying qualities for the augmented vehicle could be ensured by requiring the augmentation system to provide a match with the proven flying qualities of the DC-10. In addition, other criteria have been considered so as to add confidence in the final characteristics. Chief among these is the "Bandwidth Model" for the pitch tracking task. This criterion was originally developed by Calspan (reference 5) and has been modified and adopted by Douglas for use in transport design work. The Douglas work is reported in reference 6 and the criterion is depicted in figure 18. Briefly, the criterion considers the amount of compensation the pilot must apply to achieve a given level of pitch tracking performance without encountering pilot-induced-oscillation tendencies. The type of aircraft response to be expected from pilot commands is noted in each section of the figure. While this criterion is used for both landing approach and cruise flight conditions, there is slightly less confidence when applied to cruise cases, particularly in the left side of the diagram where few data are yet available to construct the boundaries.

Simulator Tests

The test utilized the large flight envelope data previously developed; thereby simulated flight was permitted through most of the flight envelope as well as flap, slat, and landing gear extension and retraction. Each of the evaluation pilots became familiar with the basic configuration (center of gravity at 25 percent MAC) by performing approaches, landings, go-arounds, climbs to altitude, maneuvers at altitude, descents, and stalls. To gain additional familiarization, the pilots repeated the process for an aft center-of-gravity case (cg at 40 percent MAC). No pilot ratings were taken during this portion of the experiment, but pilot comments were solicited. From the commentary, it was determined that the remainder of the test should concentrate on the landing approach and on the cruise flight condition.

In the formal evaluations, the matrix of test configurations consisted of the 15 possible combinations of five center-of-gravity locations (25, 35, 40, 45, and 50 percent MAC) and three horizontal tail sizes (100, 85, and 70 percent of nominal). Variations in tail size were included in an attempt to identify problems that might be attributed to deficient pitch control at various stability levels. Runs were conducted at each of the two flight conditions with both moderate atmospheric turbulence and smooth air. The description of turbulence here refers to the pilot assessment, which reflects the attenuation of total aircraft motion felt in the cockpit. The actual input turbulence was a level described as "moderate-to-heavy." The intensity of the turbulence is described by a vertical gust component (root mean square) of 2.13 m/s (7 ft/sec) in the landing approach, and 1.52 m/s (5 ft/sec) in the cruise. The turbulence model used is reported in Reference 7.

Some preliminary results are available from the experiment. In general, the landing approach case was critical so most of the analysis has focused in this area. Mean values of pilot ratings (using the Cooper-Harper scale given in figure 18) are shown as a function of static margin in figure 19. These data are for the case of moderate atmospheric turbulence. Although there is considerable scatter in the data, they suggest that the limiting static margin for pilot acceptability is about a negative 4 or 5 percent MAC: i.e., where the mean pilot ratings exceed a value of 6.5. The fact that the mean pilot

ratings in the stable area are poor is attributed to two causes: the presence of moderate turbulence and unsatisfactory lateral-directional characteristics of the simulated aircraft. For the second reason, all the pilot ratings may tend to be slightly higher (worse) than they should be, in which event a minimum static margin of negative 4 or 5 percent MAC may be on the conservative side. Figure 19 provides an indication of the effect of more satisfactory lateral-directional characteristics. This suggests a static margin of negative 8 or 9 percent MAC would be acceptable.

Improved lateral-directional characteristics will be incorporated in a future motion base simulator experiment.

The pilot ratings have been compared with the "Bandwidth Model" previously mentioned and are presented in figure 20. Again, the landing approach case with turbulence is shown. Excellent correlation is apparent, particularly when the poor lateral-directional characteristics are considered. If the pilot ratings were to be reduced (improved) slightly to account for this effect, even better agreement would be achieved. It is estimated that in the region of interest the pilot ratings would be reduced (improved) by approximately one unit due to the improved lateral-directional characteristics. Additional confidence has therefore been furnished for the continued use of this criterion, both for the unaugmented aircraft (Level 2) and the augmented aircraft (Level 1).

CONCLUDING REMARKS

For technology development toward advanced derivatives of the DC-10, Douglas is active in specific fields under the ACEE Energy Efficiency Transport program. These fields are the wind tunnel development at high and low speed of high-aspect-ratio supercritical wing designs, and the design of a longitudinal stability augmentation system. Also included is the design of an optimized wing-winglet combination.

The design work leading to the model development for the high-aspect-ratio supercritical wing has benefitted from the use of new and sophisticated analytical tools which show good agreement with test data. The use of these methods to study a wide range of variables will result in wind-tunnel tests of models much closer to the final configuration.

The determination of acceptable levels of flying quality is a prerequisite for the design in a failure condition of the longitudinal stability augmentation system. In normal operation, the system design will provide a quality similar to a proven high standard, such as the DC-10. Pilot simulator tests have been completed to demonstrate the effects of alternative levels of flying quality, and perhaps more importantly suggest criteria by which these levels may be measured. A further group of tests is planned, which will expand the scope to include control system investigation.

REFERENCES

1. Whitcomb, Richard T.: Review of NASA's Supercritical Wing Airfoils. 9th Congress International Council of Aeronautical Sciences, Haifa, August 1974.

2. Jameson, A.; and Caughey, D. A.: Numerical Calculation of Transonic Flow Past a Swept Wing. New York University DRDA Report C003077-140, May 1977.

3. Cooper, G. E.; and Harper, R. P.: The Use of Pilot Rating in the Evaluation of Aircraft Handling Qualities. NASA TN D-5153, April 1969.

4. Military Specification, Flying Qualities of Piloted Airplanes. MIL-F-8785B (ASG), 7 August 1969.

5. Neal, T. P.; and Smith, R. E.: An In-Flight Investigation to Develop Control System Design Criteria for Fighter Airplanes. AFFDL-TR-70-74, Vol 1, December 1970.

6. Richard, W. W.: Longitudinal Flying Qualities in the Landing Approach. Douglas Aircraft Company, Douglas Paper 6469, May 1976.

7. Barr, N. M.; Gangass, D.; and Schaeffer, D. R.: Wind Models for Flight Simulation and Certification of Landing and Approach Guidance and Control Systems. FAA-RD-74-206, December 1974.

TABLE 1
COMPARISON OF CONFIGURATION USING ADVANCED
OR CONVENTIONAL HIGH-LIFT SYSTEMS

	ADVANCED		CONVENTIONAL	
WING AREA	202.99 m^2	(2,185 FT^2)	205.32 m^2	(2,210 FT^2)
TOGW	137,393 kg	(302,900 LB)	138,073 kg	(304,400 LB)
OWE	81,627 kg	(179,956 LB)	82,135 kg	(181,077 LB)
INITIAL CRUISE ALTITUDE	10,363 m	(34,000 FT)	10,424 m	(34,200 FT)
$V_{APPROACH}$	61.9 m/s	(120.4 KEAS)	64.8 m/s	(126 KEAS)
TOFL	1,768 m	(5,800 FT)	2,179 m	(7,150 FT)

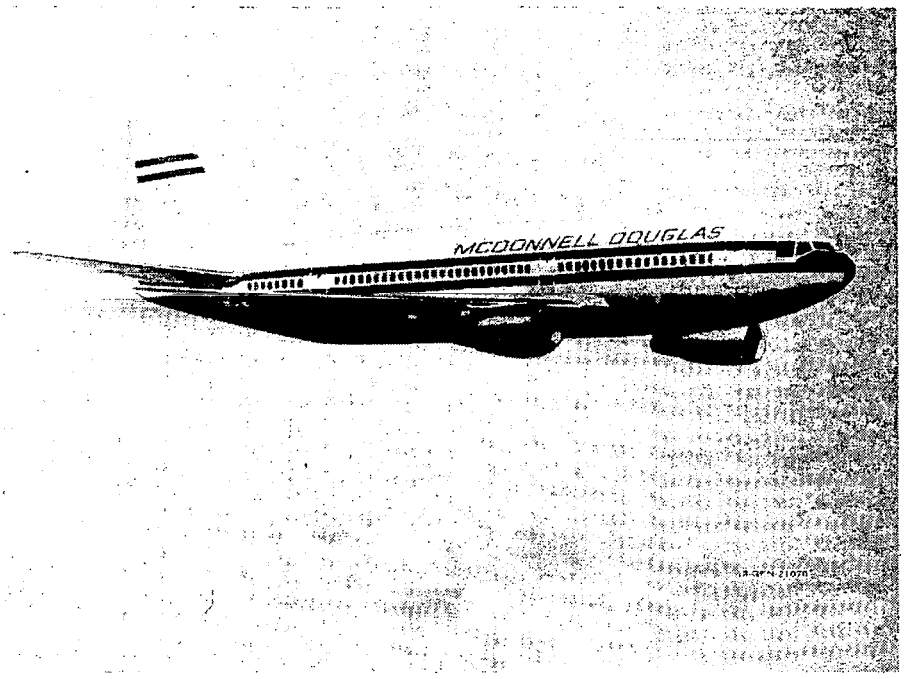

Figure 1.- Douglas DC-X-200 transport.

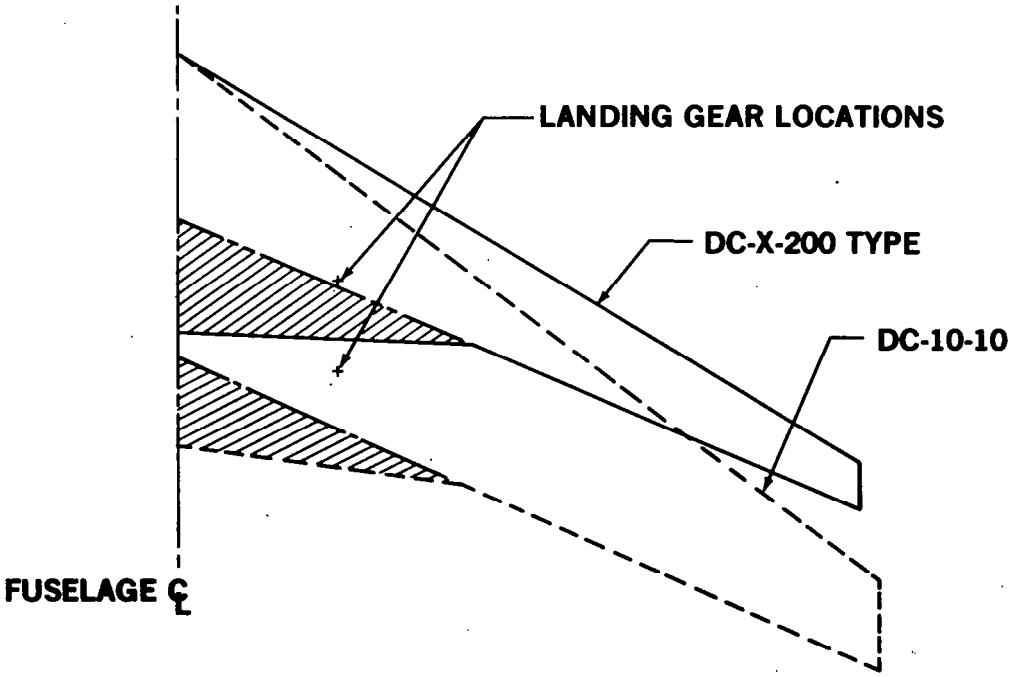

Figure 2.- Planform comparison.

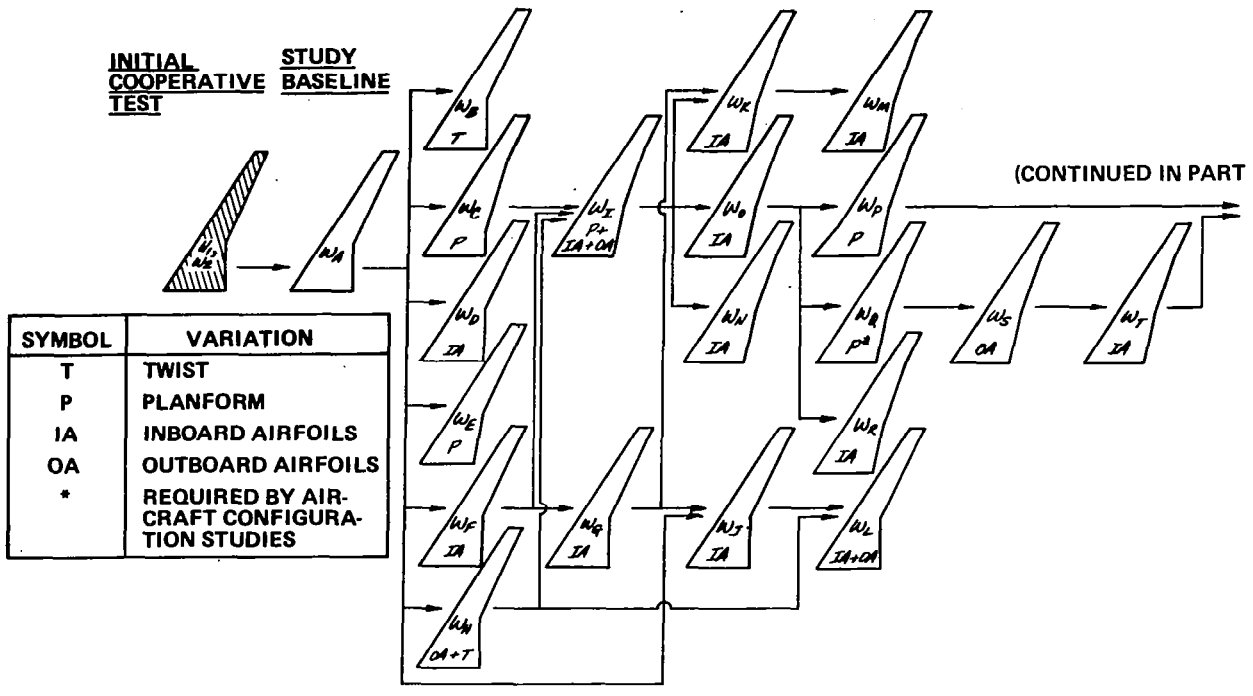

Figure 3.- Wing development matrix (Part 1).

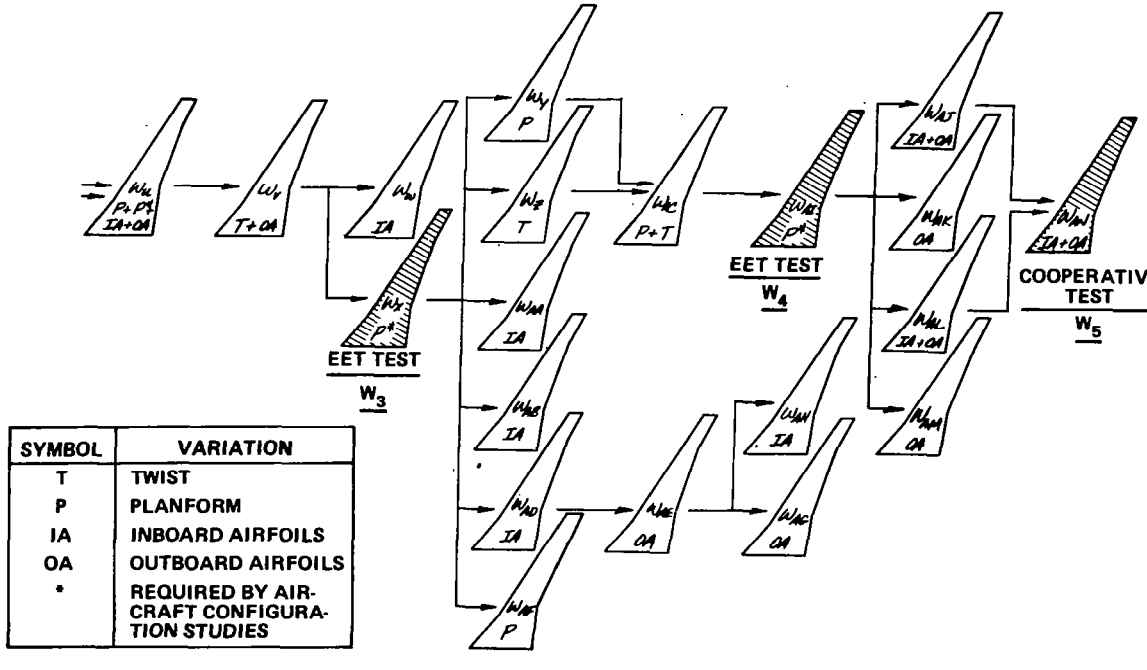

Figure 4.- Wing development matrix (Part 2).

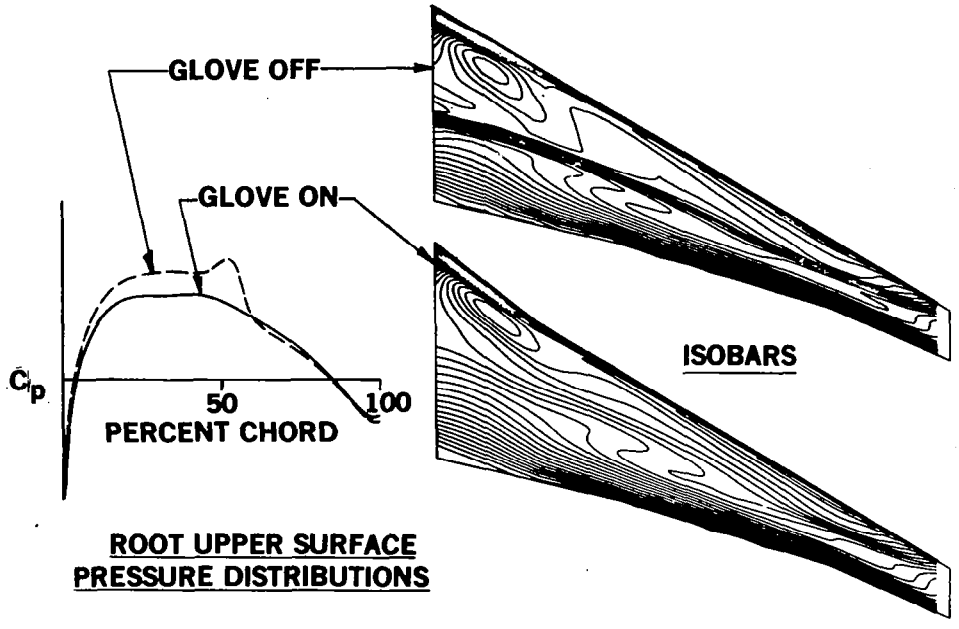

Figure 5.- Effect of inboard leading-edge glove.

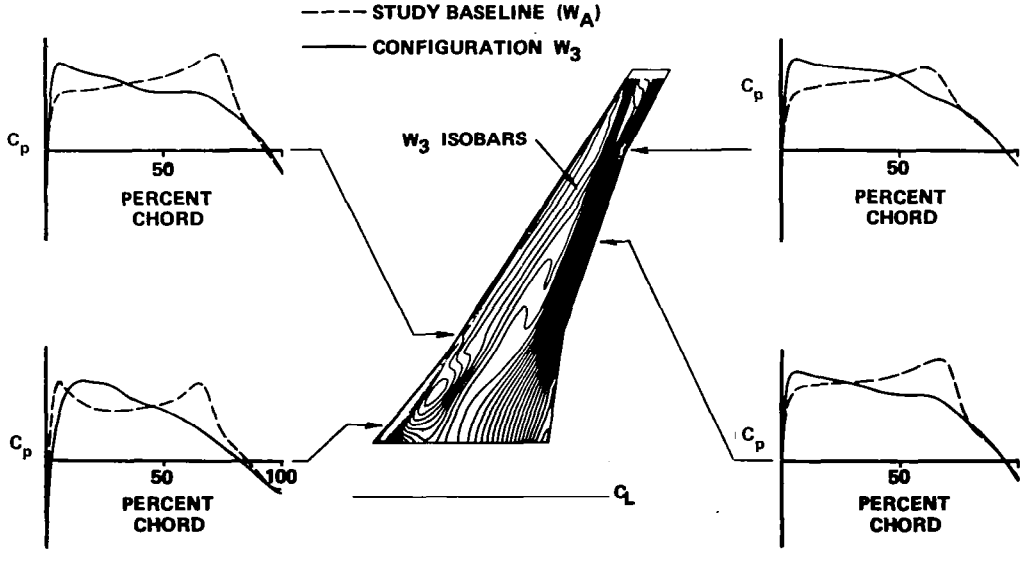

Figure 6.- Comparison of study baseline and configuration W_3 upper baseline pressure distributions.

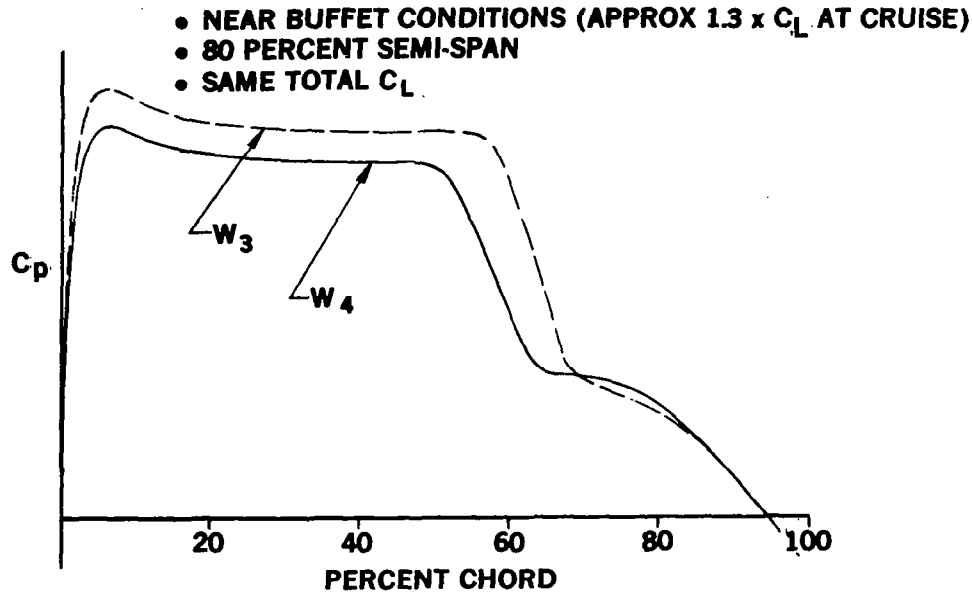

Figure 7.- Comparison of upper-surface chordwise pressure distributions for wings W_3 and W_4.

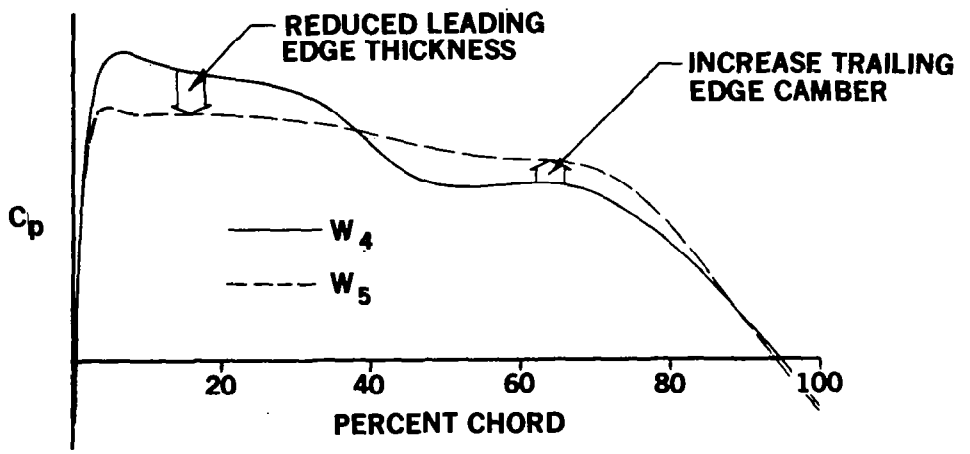

Figure 8.- Comparison of upper-surface chordwise pressure distributions for wings W_4 and W_5.

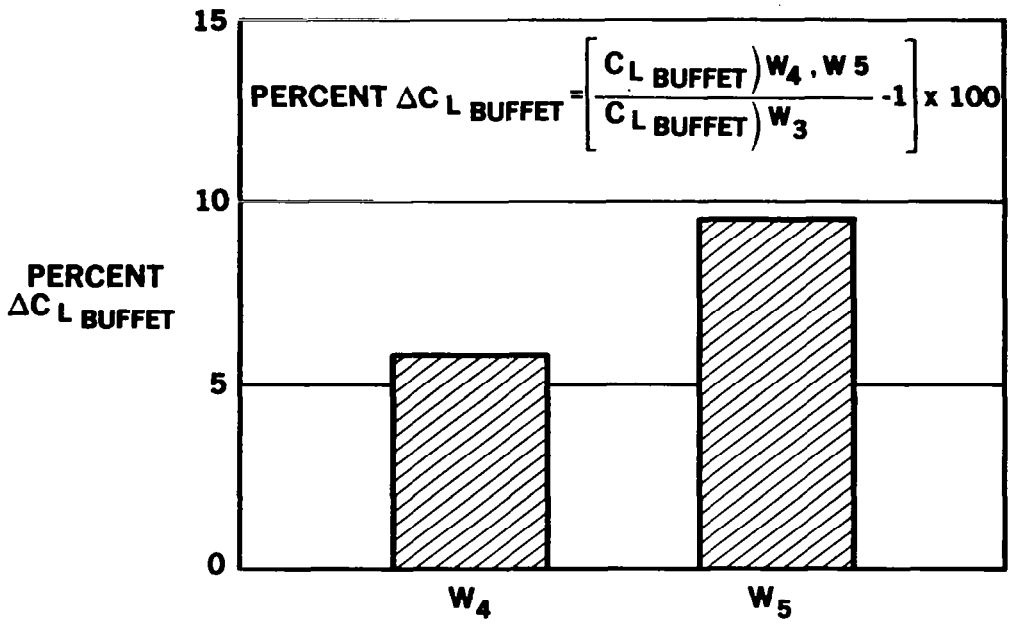

Figure 9.- Estimated $C_{L_{BUFFET}}$ improvement.

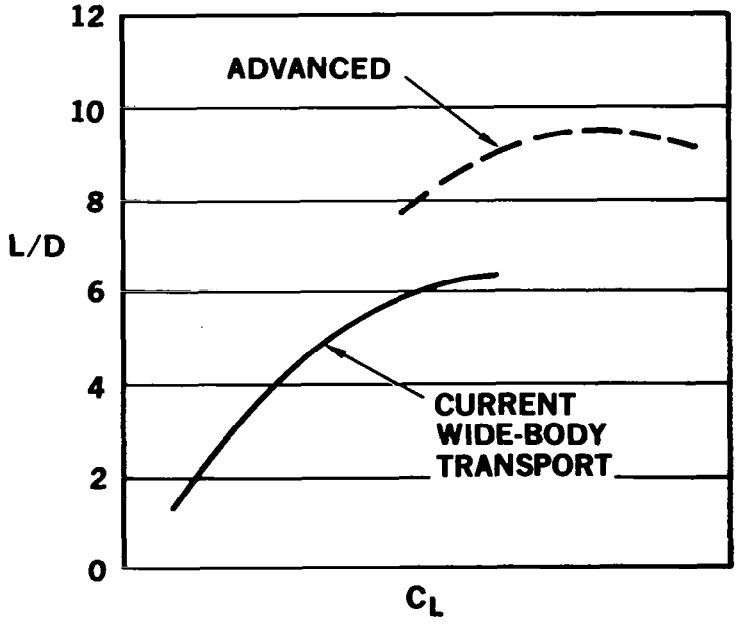

Figure 10.- Comparison of current wide-body and advanced high-aspect-ratio SCW transport landing L/D characteristics.

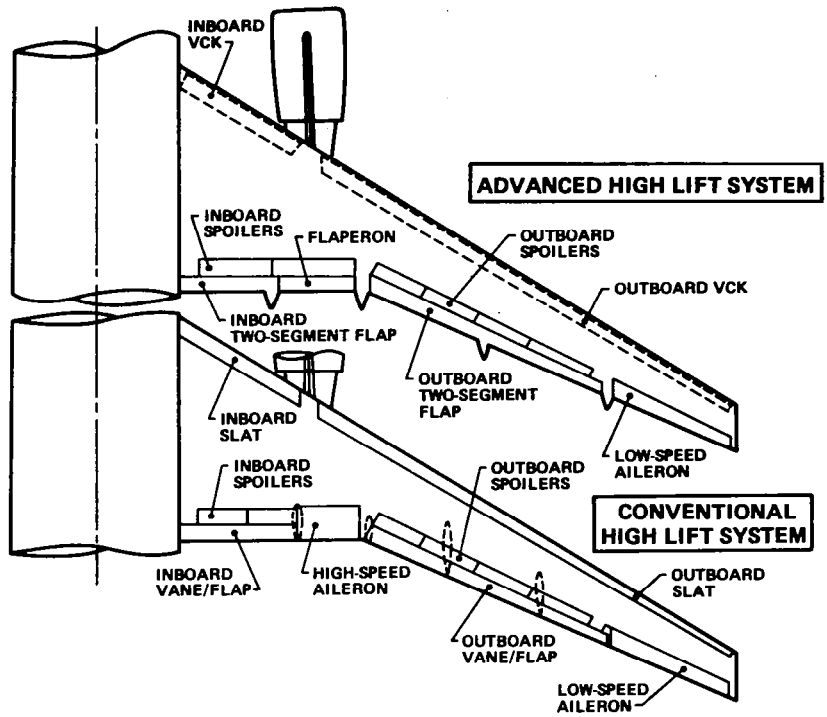

Figure 11.- High-lift system configuration comparison.

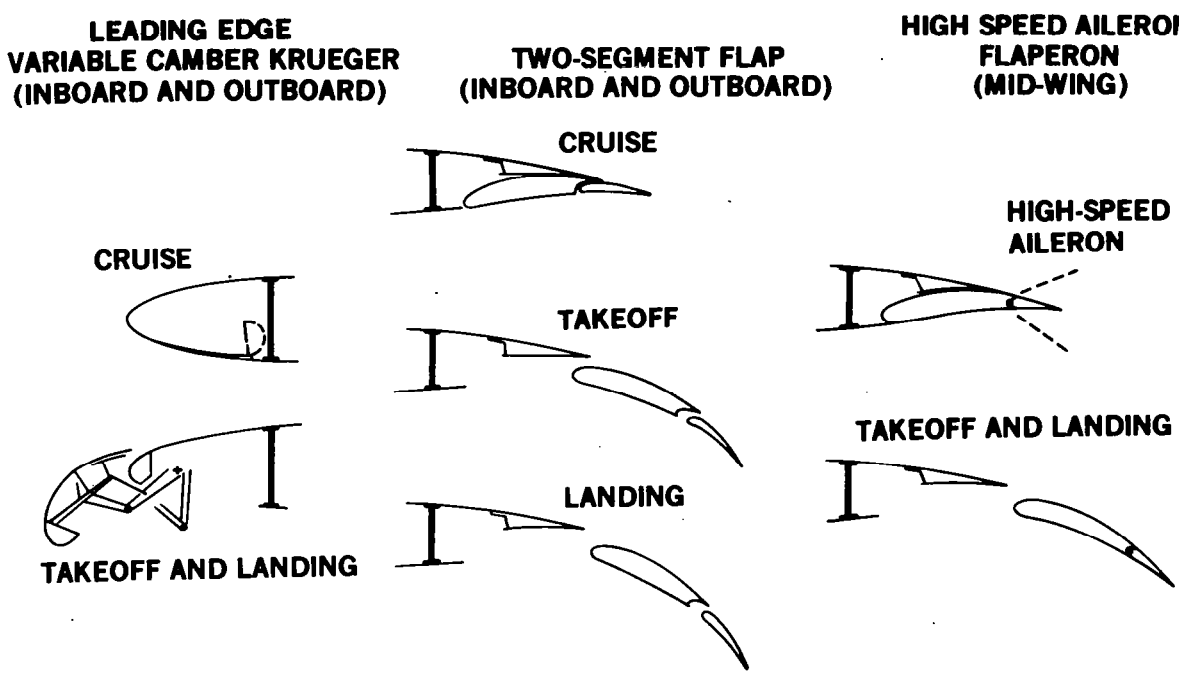

Figure 12.- Advanced high-lift system chordwise sections.

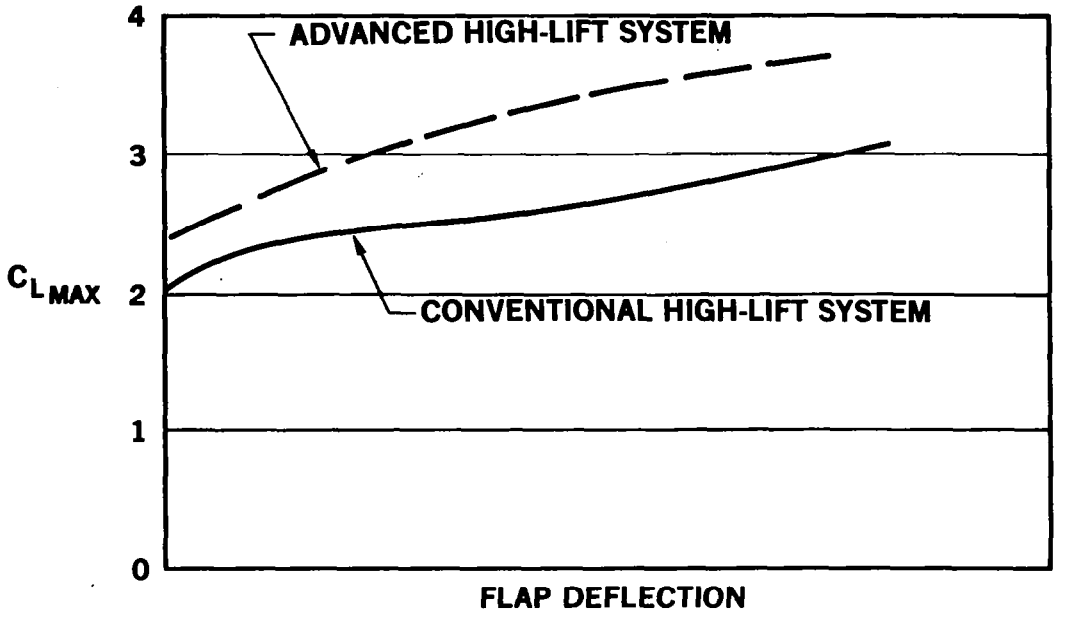

Figure 13.- Comparison of conventional and advanced high-lift system $C_{L_{MAX}}$ characteristics.

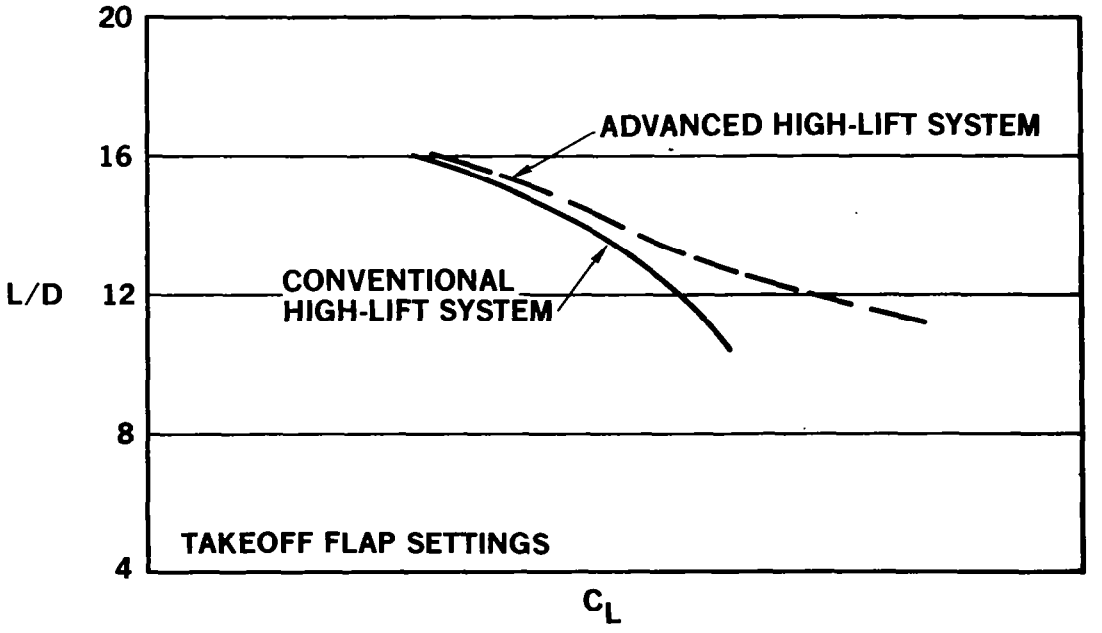

Figure 14.- Comparison of conventional and advanced high-lift system takeoff L/D characteristics.

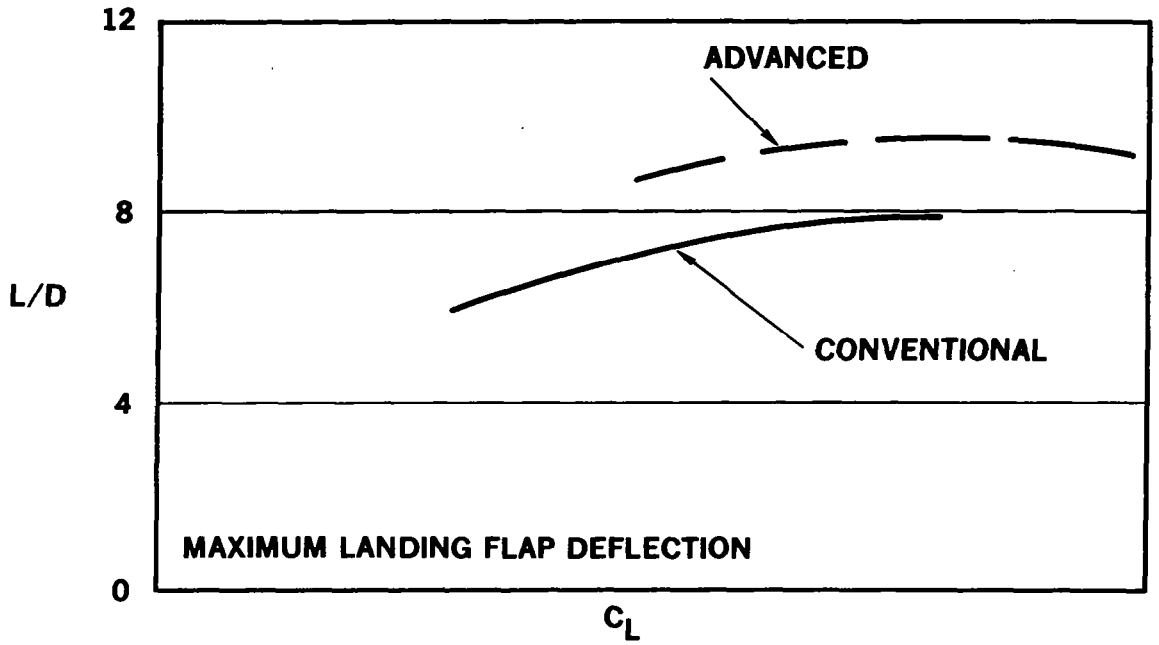

Figure 15.- Comparison of conventional and advanced high-lift system landing approach L/D characteristics.

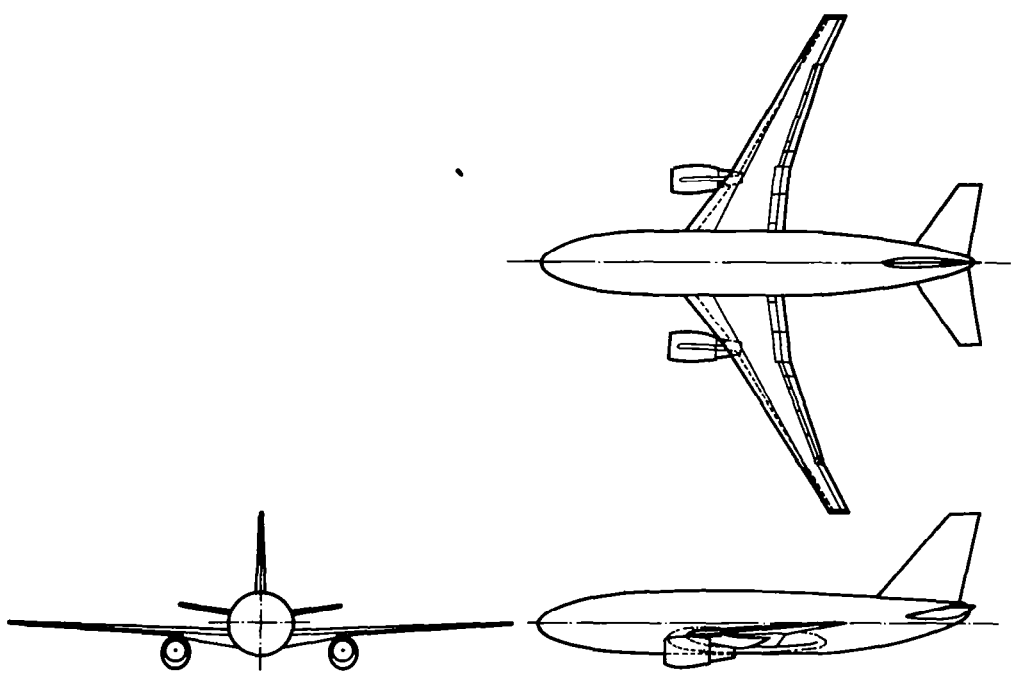

Figure 16.- High-lift, low-speed wind-tunnel model.

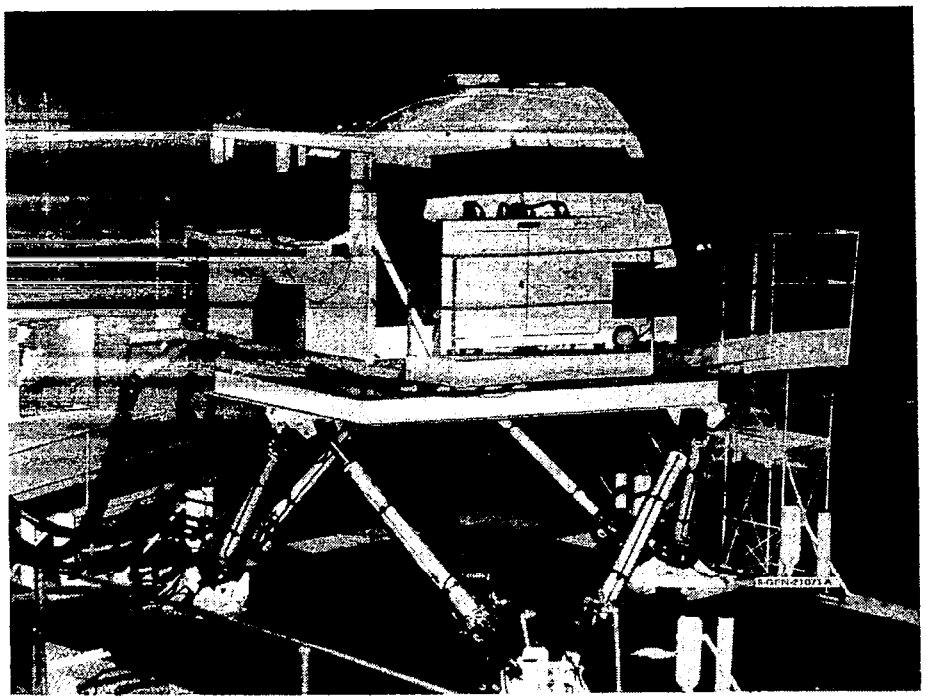

Figure 17.- Douglas six-degree-of-freedom motion simulator.

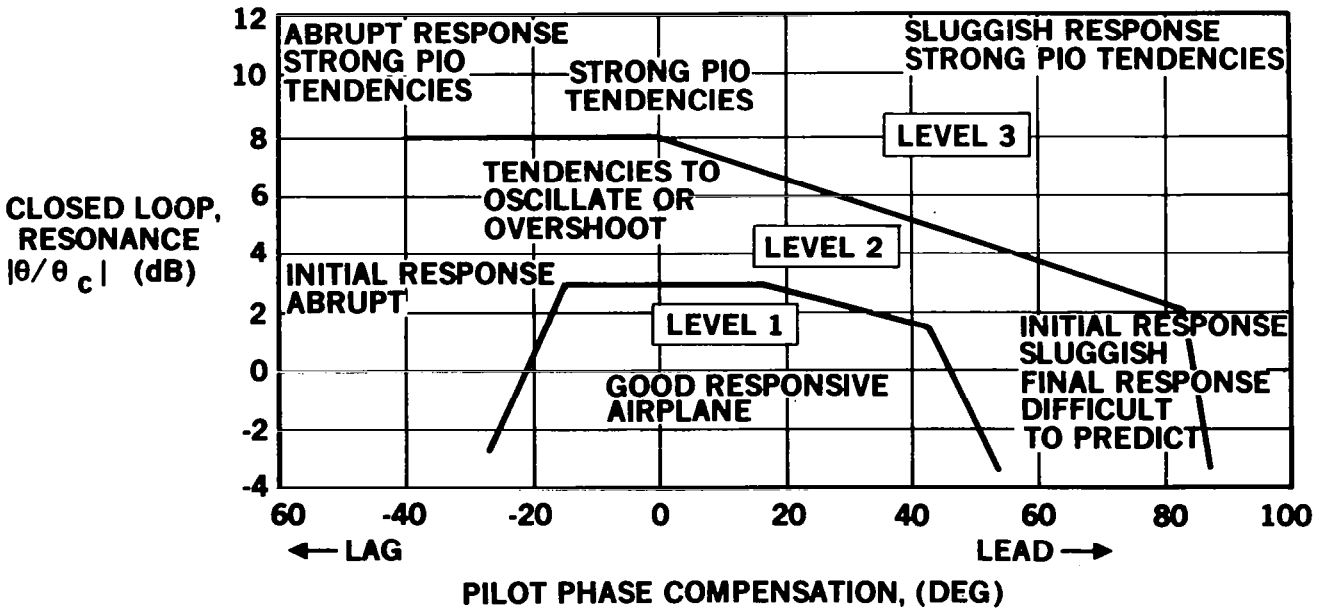

Figure 18.- Pitch tracking criterion.

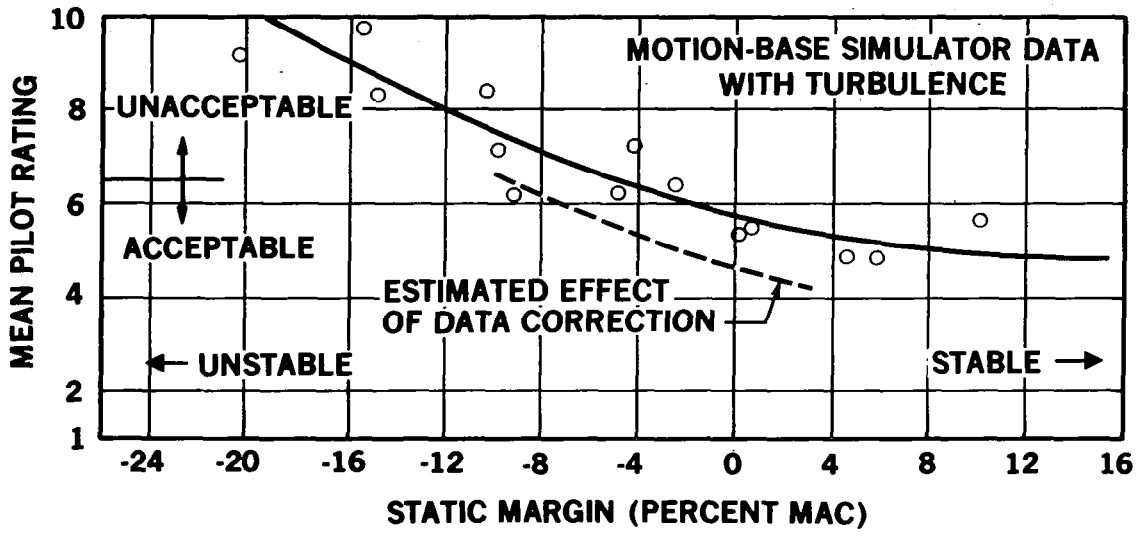

Figure 19.- Pilot acceptance of static instability — landing approach.

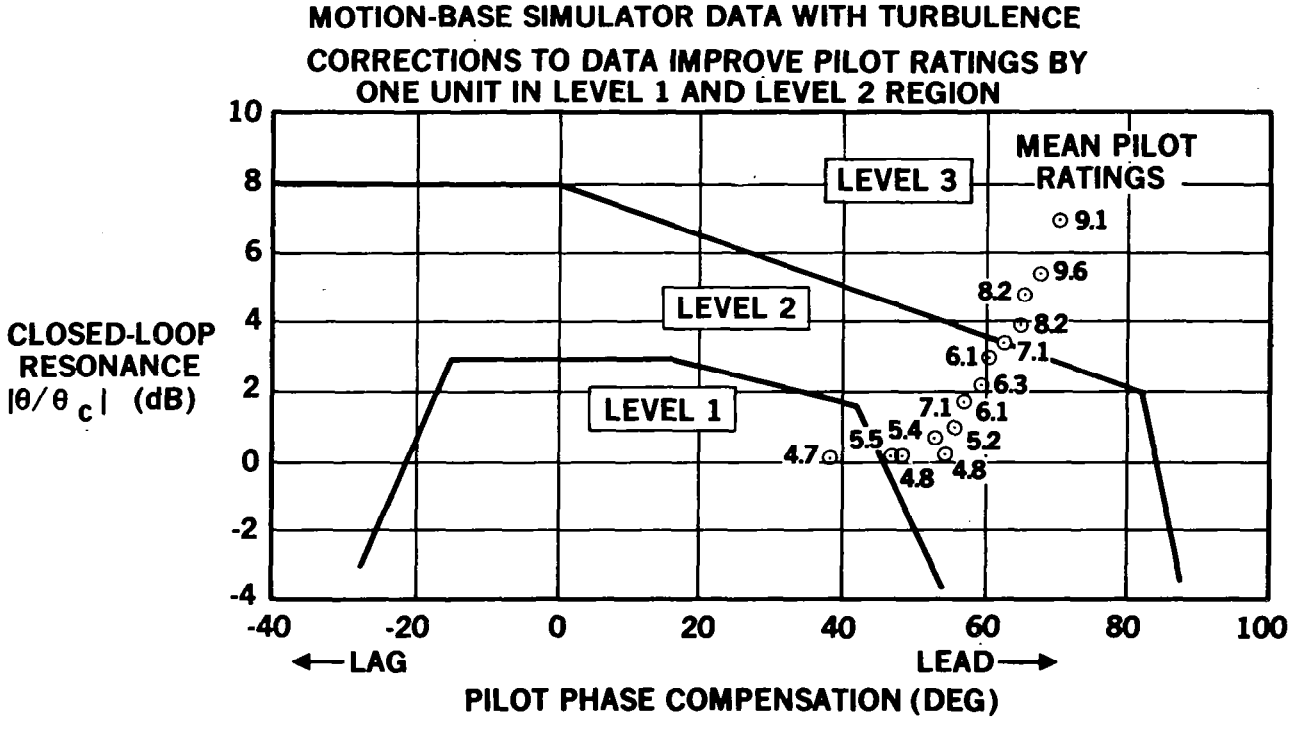

Figure 20.- Landing approach pitch tracking criterion.